New dynamic model for a Ballbot system

Andrea Bonci *Member, IEEE*
Dip. Ingegneria dell'Informazione (DII) - Università Politecnica delle Marche 60131 Ancona, Italy
Email: a.bonci@univpm.it

***Abstract*—A Ballbot is a self-balanced mobile robot designed for omnidirectional mobility. The structure self-balanced on a ball giving to the system only one contact point with the ground. In this paper the dynamical model of a Ballbot system is investigated in order to find a linearized model which is able to describe the three-dimensional dynamics of the mechatronic system by a simpler set of equations. Due to the system's complexity, the equations of motion are often obtained by the energy method of Lagrange, they consist of a vast nonlinear ordinary differential equations (ODE), which are often numerically linearized for small perturbations. The present paper proposes to model the whole 3D dynamics of the Ballbot with the Newton-Euler formalism and Tait-Bryan angles in order to describe the model in terms of the system's physical parameters without resorting to numeric solution. This physical modelling is introduced to allow the simplification of the dynamic motion control of the ballbot.**

I. Introduction

The ballbot is considered a great innovation in the field of the dynamically unstable system. This kind of vehicle presents the ability to balance itself dynamically on a single spherical wheel (i.e. a ball). Unlike two-wheeled balancing mobile robots (i.e. Segway), ballbot is omni-directional and is able to roll in any direction. It has no minimal turning radius and does not have to yaw in order to change direction. The ballbot forms an underactuated system (there are more degrees of freedom than independent control inputs) where the ball is directly controlled by actuators, while the body has no direct control. It is kept upright around its unstable equilibrium point by the control applied to the ball, therefore the ballbot can be considered and modeled using a similar principle as the inverted pendulum. The system is mainly composed by three parts: the body, the propulsion and the ball. The most complex part is the propulsive subsystem, which is composed of the ball actuated by three omniwheels or by four wheels (depending on the actuation system used) driven by motors. The motors gives the actuation to the ball which gives a propulsion to the system, allowing its movement. In this paper a dynamical model of the Ballbot actuated by 3 omniwheels, based on Newton-Euler formalism and Tait-Bryan angles, is presented. With this approach it is possible to describe the 3D system dynamic linearized at zero with three subsystems for the body and two subsystems for the ball having completely known parameters in terms of the system's physical parameters and no numerical approximations are reported. This leads to a more understandable physical system. The linearization of the model around the zero equilibrium point allows to obtain a linear system with reduced complexity w.r.t. the nonlinear one. The modelling technique also allows a linearization around an arbitrary equilibrium point (not addressed here). The proposed model also shows how it is possible to reduce the system's nonlinear algebric equations to ODE. Also important properties of the linearized system's model are demonstrated. The paper is organized as follows: section II summarizes the state of the art on ballbot system, section III briefly describes the mechatronic system, section IV describes the physical system, section V introduces the propulsion model, section VI computes the nonlinear equations with the Newton-Euler method, section VII summerizes all the equations, section VIII describes the linearized system and section IX concludes the paper.

II. Related works

Since the development of the automation field, the movement of complex mechatronic system has been a major feature for developers. Nowadays there are several kind of robots capable of attempting that. The most known are the anthropomorphic systems, however they present an high level of complexity due to the high number of actuators. Obviously this affects the costs of realization and, moreover, the consumption of energy reducing the usage-time of the robot. Therefore the study of systems with a fewer number of actuator has begun. Among them, the most known and commercialized are the Segways. This kind of system consists of two-wheeled self-balancing robot, which has been developed in several ways by different researchers. This vehicle allows an higher durability with respect to the anthropomorphic system, however it needs at least twice the space of his body to execute complex movements. This is the main reason that has lead to the realization of a ball based system, in which every movement can be done occupying just the space of its body structure. The first ballbot was a four wheel robot developed in 2006 at Carnegie Mellon University (CMU) in the USA ([1], [2]). A different one having a propulsion system based on three omniwheels and stepper motors has been developed by Tohoku Gaku in University (TGU) in Japan [3]. Another one having four wheels and based on Lego mindstorms has been presented as student project at University of Adelaide (UA) in Australia [4]. A further development about the propelling with three omniwheels has been proposed in the bachelor thesis of ETH Zurich [5], where a Lagrangian approach has been selected for modelling and a numerical approximation has been used to synthetize the linearized model due to the difficulty in linearizing a large number of nonlinear equations.

9978-1-5090-6190-7/16/$31.00 © 2016 IEEE

During the last years further works have been proposed in literature for different issues [6] [7]. Few of them often cope with modelling and often simplifying assumptions on model dynamic have been made, e.g. decoupling motion in 3D planes. In the follows a different approach to model this case of study is proposed.

III. The mechatronic ballbot system

Fig. 1. Mechatronic system

Main mechanical data	
Description	Value
Mass of the ball	0.65$[kg]$
Mass of the wheel	107$[g]$
Mass of the body	5.045$[kg]$
Radius of the ball	120 $[mm]$
Radius of the wheel	53 $[mm]$
Radius of the body	140 $[mm]$
Height from the center of mass	410 $[mm]$
Inertia of the ball	0.005$[kgm^2]$
Inertia of the body	0.47$[kgm^2]$

TABLE I. System parameters

In this section the structure of the mechatronic system is introduced. As shown in figure 1, it is basically composed of 3 parts: the chassis (the body), the propulsion system and the ball. The whole structure is made of alluminium and plexiglass, in order to keep the system as light as possible. The chassis is composed of 3 parallels circular plates placed at 100 mm. On the bottom of the middle level is placed the Inertial Measurement Unit (IMU), a triple axis accelerometer and gyro MPU6050 by Invense Sense. The propulsion system is mainly composed of the motor (Pololu 1446), the omnidirectional wheels and the motor driver (a 10 A 3$-$25 V motor controller). This kind of wheels allow the structure to develop a tangential force in the direction of movement to his own circumference. Moreover it allows the system to slip sideways, if some longitudinal force is applied. The wheels present an angle α of $40°$ between their bottom and the centre of the ball as shown in 2b. This is the minimum angle that allows the structure to not slip over the ball. The system uses three 12 V brushed DC motor with a 102.083 : 1 metal gearbox and an integrated quadrature encoder that provides a resolution of 64 counts per revolution of the motor shaft, which corresponds to 6533 counts per revolution of the gearboxes output shaft. They are installed with an angle β of $120°$ between them, as shown in figure 2a. All the system is controlled by a Renesas RX 63N board with an high-performance microcontroller, incorporating an RX 600 MCU core. The main information about the physical dimension of the structure are reported in the table I.

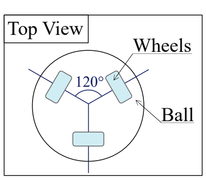

(a) *Angle between motors.*

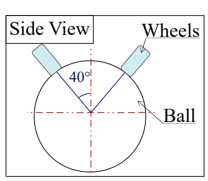

(b) *α angle.*

Fig. 2. Angles of motors and wheels

IV. Physical description of model

This section provides the specific model information of the Ballbot system. The system is assumed to be made-up of two rigid bodies: the ball and the main body (pendulum-like) provided with three actuating wheels which allow the ball to move in any direction.

A. Assumptions

In this subsection we focus on the main assumptions:

- The ball (B) and the pendulum (P) are rigid bodies;
- three reference frames are used, one absolute (Σ_E) and two are relative: the ball frame Σ_B and the pendulum frame Σ_P;
- the centers O_B and O_P of the reference systems Σ_B and Σ_P coincide with the inertia centers of gravity (cog) of the respective rigid bodies;
- the motion equations are formulated with respect to the mobile reference frame Σ_P for the following reasons:
  - the inertia matrix is time-invariant;
  - advantage of body symmetry can be taken to simplify the equations;
  - measurements taken on-board are easily converted to body-fixed frame;
  - control forces are almost always given in body-fixed frame;
- no slip: the contact points between the ball and the ground and between the wheels and the ball are assumed to be free of slippage.
- no vertical motion of the ball. The ball moves only horizontally.
- RPY (Roll Pitch Yaw) angles are assumed.

B. Coordinate systems

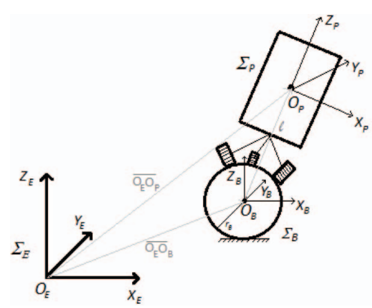

Fig. 3. Ballbot Coordinate Systems

This section briefly provides the specific description of the coordinate systems used to model the Ballbot in the Newton-Euler formalism. Figure 3 shows the reference frames and the main vectors used to model the Ballbot system. In that figure:

- $\Sigma_E = \{O_E, \widehat{i}_E, \widehat{j}_E, \widehat{k}_E\}$ is the fixed reference frame;
- $\Sigma_B = \{O_B, \widehat{i}_B, \widehat{j}_B, \widehat{k}_B\}$ is the ball reference frame, it moves with the ball but it has a fixed orientation w.r.t. Σ_E;
- $\Sigma_P = \{O_P, \widehat{i}_P, \widehat{j}_P, \widehat{k}_P\}$ is the pendulum reference frame, it moves with the center of gravity (cog) of the main body;
- $\Sigma_{W_i} = \{O_{W_i}, \widehat{i}_{W_i}, \widehat{j}_{W_i}, \widehat{k}_{W_i}\}$ is the i^{th}-wheel's reference frame, its center is fixed in the center of the i^{th} omniwheel and its x-axis is oriented towards the center of the wheel.

Here it has been assumed that:

- Σ_P has 6 degree of freedom (DoF);
- Σ_B has 2 DoF when the ball is moving on a not tilted plane.

The set of RPY angles [8] are here considered to represent the orientation configuration of the generic rigid body respect to a reference frame. By assuming the counterclockwise of rotation as positive, the sequence of elementary rotations for RPY angles are described by the rotation matrices:

$$R_x(\phi) = \begin{bmatrix}1 & 0 & 0\\ 0 & C_\phi & -S_\phi\\ 0 & S_\phi & C_\phi\end{bmatrix} R_y(\theta) = \begin{bmatrix}C_\theta & 0 & S_\theta\\ 0 & 1 & 0\\ -S_\theta & 0 & C_\theta\end{bmatrix} R_z(\psi) = \begin{bmatrix}C_\psi & -S_\psi & 0\\ S_\psi & C_\psi & 0\\ 0 & 0 & 1\end{bmatrix} \quad (1)$$

where $C_k = \cos k$, $S_k = \sin k$ and ϕ, θ, ψ are respectively the roll, pitch and yaw angles. This rotations can be used to place the 3D model in any orientation. The direction cosine matrix $R(\phi, \theta, \psi)$ is obtained by post-multiplying:

$$R(\phi, \theta, \psi) = R_z(\psi) R_y(\theta) R_x(\phi). \quad (2)$$

The notation used in the following will identify X_α^β as the geometric operator X which transforms the coordinates of a generic vector in the reference frame Σ_α into the coordinates of the reference frame Σ_β. According to this notation we define the following vectors:

vector	description
$\Gamma_P^E = \overline{O_E\, O_P} = [x, y, z]^T$	position of the pendulum's cog w.r.t. Σ_E
$\Theta_P^E = [\phi, \theta, \psi]^T$	orientation of Σ_P axes w.r.t. Σ_E
$\Gamma_B^E = \overline{O_E O_B} = [x_B, y_B, z_B]^T$	position of the ball's cog w.r.t. Σ_E
$\Theta_B^E = [\phi_B, \theta_B, \psi_B]^T$	ball's rotation angles w.r.t. Σ_E
$V_P = [u, v, w]^T$	velocities of the pendulum in Σ_P
$\omega_P = [p, q, r]^T$	angular velocities of the pendulum in Σ_P
$V_B = [u_B, v_B, w_B]^T$	velocities of the ball in Σ_B
$\omega_B = [p_B, q_B, r_B]^T$	angular velocities of the ball in Σ_B
I_P	inertia tensor of the pendulum
I_B	inertia tensor of the ball
M_P	pendulum angular momentum
$L = [0, 0, -l]^T$	position vector of the ball's cog w.r.t. Σ_P
$R_B = [0, 0, -R_b]^T$	position vector of the ground contact point w.r.t. Σ_B
$G_B^E = [0, 0, -m_b g]^T$	vector potential force of the ball
$G_P^E = [0, 0, -m_p g]^T$	vector potential force of the pedulum
$R_t = [r_{t_x}, r_{t_y}, r_{t_z}]^T$	ball-ground reaction forces
$R_v = [r_{v_x}, r_{v_y}, r_{v_z}]^T$	ball-pendulum reaction forces

TABLE II. vectors

symbol	description
m_b	mass of the ball
m_p	mass of the pendulum (body)
R_b	radius of the ball
R_w	radius of the wheel
l	distance of ball-pendulum cogs
g	gravitational acceleration
$I_{b_x} = I_{b_y} = I_{b_z} \triangleq I_b$	ball moment of inertia
$I_{p_x} = I_{p_y} \triangleq I_p$	pendulum moment of inertia w.r.t. x, y axes
I_{p_z}	pendulum moment of inertia w.r.t. z axis
α	angle between the wheel's contact point and the center of the ball
β	angle between the motors

TABLE III. physical parameters

By using the previous formalism, the rotation matrices used in the next sections are introduced:

- $R_P^E = R(\phi, \theta, \psi) = R_z(\psi) R_y(\theta) R_x(\phi) =$ direction cosine matrix (2) from Σ_P to Σ_E;
- $R_B^P = R_x^T(\phi) R_y^T(\theta)$, rotation matrix from Σ_B to Σ_P;
- $R_{W_i}^P = R_z(\beta) R_y(\alpha) =$ rotation matrix from Σ_{W_i} to Σ_P.

Later in the paper the physical parameters listed in table III will be used to model the dynamic behaviors.

V. The propulsion system and the input torques

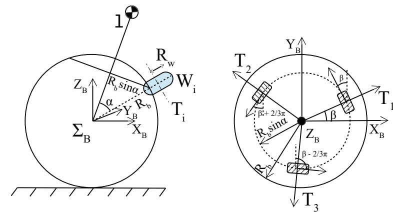

Fig. 4. Side and above view of the geometry between ball and wheels

The present section is devoted to the modelling of the torques supplied by the omniwheels to the ball. Denoting with U the effective vector torque applied by the omniwheels to the ball and with $\overline{U} = [u_x\ u_y\ u_z]^T$ the vector torque available at the omniwheels, the following relation can be written:

$$U = k\overline{U}, \quad k = \frac{R_b}{R_w}, \quad (3)$$

where k is the ratio between the torques (or the ratio between the angular velocities) among the ball and the wheels, which are derived by $R_w \omega_W = R_b \omega_B$ and $\omega_W \tau_W = \omega_B \tau_B$. Each omniwheel $W_i, i = 1, \ldots, 3$ is actuated by its own motor drive. Denoting with T_i the motor torque of the i^{th} omniwheel W_i, then according to the physical configuration of the omniwheels showed in figure 4, the vector $\overline{U}$ can be expressed as:

$$\overline{U} = R_{W_1}^P(\alpha, \beta) \begin{bmatrix}T_1\\0\\0\end{bmatrix} + R_{W_2}^P(\alpha, \beta + \tfrac{2}{3\pi}) \begin{bmatrix}T_2\\0\\0\end{bmatrix} + R_{W_3}^P(\alpha, \beta - \tfrac{2}{3\pi}) \begin{bmatrix}T_3\\0\\0\end{bmatrix} \quad (4)$$

which results in:

$$\overline{U} = \begin{bmatrix}u_x\\u_y\\u_z\end{bmatrix} = \begin{bmatrix}C_\alpha(T_1 C_\beta + C_{\beta+\frac{2}{3\pi}} + T_3 C_{\beta-\frac{2}{3\pi}})\\ C_\alpha(T_1 S_\beta + S_{\beta+\frac{2}{3\pi}} + T_3 S_{\beta-\frac{2}{3\pi}})\\ -S_\alpha(T_1 + T_2 + T_3)\end{bmatrix}. \quad (5)$$

VI. Non-linear dynamic model using Newton-Euler method

In this work the Newton-Euler method and the Tait-Bryan angles theories have been used instead of the Lagrangian method, in order to find the equations of motion for the Ballbot system. The model has been developed as follows: by assuming the ballbot consisting of two rigid bodies, for each rigid body the kinematic equations of both linear and angular velocities are firstly derived, later the translational and rotational dynamic of these bodies are computed from the Euler's axioms of the Newton second law; besides, the geometric and the kinematic binding equations between the rigid bodies are added to the model. Finally the external forces/torques are defined and included in the model with the actuation torques.

A. Kinematics

The ballbot kinematics is related to the velocities of its rigid bodies, in the following, for each rigid body (pendulum and ball) translational and angular velocities are derived.

1) Pendulum Kinematics: the linear velocity V_P and the angular velocity ω_P, referred to Σ_P are here transformed in velocities related to Σ_E:

$$\begin{cases} \dot{\Gamma}_P^E = R_P^E V_P \\ \dot{\Theta}_P^E = T_\Theta^{-1}\omega_P, \end{cases} \tag{6}$$

where R_P^E is the direction cosine matrix (2) and T_Θ^{-1} is the matrix which relate the angular velocity in Σ_E [9] (or Euler rates) to the angular velocity in ω_P, defined as:

$$T_\Theta^{-1} = \begin{bmatrix} 1 & S_\phi T_\theta & C_\phi T_\theta \\ 0 & C_\phi & -S_\phi \\ 0 & \frac{S_\phi}{C_\theta} & \frac{C_\phi}{C_\theta} \end{bmatrix} \tag{7}$$

2) Ball Kinematics: referring to Σ_B the ball linear velocity V_B and angular velocity ω_B are transformed into velocities related to Σ_E:

$$\begin{cases} \dot{\Gamma}_E^B = R_Z(\psi) V_B \\ \dot{\Theta}_E^B = R_Z(\psi)\omega_B. \end{cases} \tag{8}$$

B. Dynamics

In this subsection, by using the first and the second axiom of the Newton's second law, the translational and rotational dynamic equations of both rigid bodies forming the ballbot are computed and related to Σ_E:

1) Pendulum Translational Dynamics: according the first axiom of the Newton's second law the linear components of the pendulum motion have the following equations:

$$m_p \frac{d}{dt}\left(R_P^E V_P\right) = {F_{ext}}_P^E, \tag{9}$$

where m_P is the pendulum mass and ${F_{ext}}_P^E$ represents all the external forces acting on the Pendulum frame Σ_P and defined in Σ_E. Equation (9) can be written as:

$$m_p(\dot{R}_P^E V_P + R_P^E \dot{V}_P) = {F_{ext}}_P^E. \tag{10}$$

Recalling that $\dot{R}_P^E V_P = R_P^E(\omega_P \times V_P)$ and ${F_{ext}}_P^E = R_P^{E-1}{F_{ext}}_P^E$ gives:

$$m_p(\omega_P \times V_P + \dot{V}_P) = {F_{ext}}_P^P, \tag{11}$$

where ${F_{ext}}_P^P$ represents all the external forces acting on the pendulum and defined on the pendulum frame Σ_P.

2) Pendulum Angular Dynamics: from the Euler's second axiom of the Newton's second law applied to the pendulum follows:

$$\frac{d}{dt}\left(R_P^E M_P\right) = \frac{d}{dt}\left(R_P^E I_P \omega_P\right) = {\tau_{ext}}_P^E, \tag{12}$$

where I_P is the pendulum tensor of inertia, $M_P = I_P\omega_P$ is the pendulum angular momentum and ${\tau_{ext}}_P^E$ represents all the external torques acting on the pendulum frame Σ_P and defined in Σ_E. Equation (12) give rise to (14) as follows:

$$\begin{aligned} &\dot{R}_P^E(I_P\omega_P) + R_P^E\dot{\omega}_P = {\tau_{ext}}_P^E \\ &R_P^E(\omega_P \times I_P\omega_p + I_P\dot{\omega}_P) = R_P^E {\tau_{ext}}_P^P \end{aligned} \tag{13}$$

$$(\omega_P \times I_P\omega_p + I_P\dot{\omega}_P) = {\tau_{ext}}_P^P, \tag{14}$$

where ${\tau_{ext}}_P^P$ represents all the external torques acting on the pendulum and defined in Σ_P.

3) Ball Translational Dynamics: as for the pendulum the linear components of the ball motion are:

$$\frac{d}{dt}\left(m_b\dot{\Gamma}_B^E\right) = m_b\frac{d}{dt}\left(R_P^E R_B^P V_B\right) = {F_{ext}}_B^E, \tag{15}$$

where m_b is the ball mass and ${F_{ext}}_B^E$ represents all the external forces acting on the ball frame Σ_B and defined in Σ_E. Equation (15) gives rise to (17) as follows:

$$m_b(\dot{R}_P^E R_B^P V_B + R_P^E \dot{R}_B^P V_B + R_P^E R_B^P \dot{V}_B) = {F_{ext}}_B^E. \tag{16}$$

By similar operation as in (11) we have:

$$m_b(\omega_P \times (R_B^P V_B) + R_B^P(\omega_B^* \times V_B + \dot{V}_B)) = {F_{ext}}_B^P, \tag{17}$$

where the angular velocity vector $\omega_B^* = [-p, -q, 0]^T$ is the axial vector of the skew-symmetric matrix associated to the time derivation of the rotation matrix R_B^P [9]. In this case, it is better to consider the external forces acting on the ball, not related to the ball frame Σ_B but to the pendulum frame Σ_P.

4) Ball Angular Dynamics: the angular components of the Ball motion are according to the following equation:

$$\frac{d}{dt}\left(R_B^E M_B\right) = \frac{d}{dt}\left(R_B^E I_B\omega_B\right) = {\tau_{ext}}_B^E, \tag{18}$$

where I_B is the ball tensor of inertia, $M_B = I_B\omega_B$ is the angular momentum of the ball and ${\tau_{ext}}_B^E$ represents all the external torques acting on the Ball frame Σ_B and defined in Σ_E. Equation (18) gives rise to (20) as follows:

$$\begin{aligned} &\dot{R}_P^E R_B^P I_B\omega_B + R_P^E \dot{R}_B^P I_B\omega_B + R_P^E R_B^P I_B\dot{\omega}_B = {\tau_{ext}}_B^E \\ &R_P^E(\omega_P \times R_B^P I_B\omega_B) + R_P^E R_B^P(\omega_B^* \times I_B\omega_B) \\ &R_P^E R_B^P I_B\dot{\omega}_B = R_P^E {\tau_{ext}}_B^P \end{aligned} \tag{19}$$

$$\omega_P \times R_B^P I_B\omega_B + R_B^P(\omega_B^* \times I_B\omega_B) + R_B^P I_B\dot{\omega}_B = {\tau_{ext}}_B^P, \tag{20}$$

where ${\tau_{ext}}_B^P$ represents all the torques acting on the ball referred to Σ_P, and ω_B^*, as in (17).

5) Summary of dynamic equations: equations (11), (14), (17), (20) describe the dynamics of the Ballbot rigid bodies without constraints between them. From now on these four equations will be used in the dynamic motion of the ballbot system. To complete the model it is necessary to introduce a set of equations which describe:

- the system's constraints: a geometric one representing the fixed distance between the two rigid bodies and a kinematic one, representing the pure rolling constant, respectively expressed in the form of a binding equation;
- the external forces and torques acting on the pendulum and on the ball;
- the relations between: external forces and torques acting on the bodies and the input torques generated from the system's actuators (three omniwheels, each one respectively actuated by a proper DC motor).

C. Binding Equations

The Ballbot system is assumed to be composed of 2 rigid bodies: the pendulum including the three omniwheels and the ball. The motion of each one is not completely independent from the others due to existing constraints between them. The following constraints are here considered:

- a geometric constrain which represents the invariance between the position of the cog of the ball and the cog of the pendulum;
- the pure-rolling constraint between the ball and the floor.

Their equations are explained in the following:

1) Ball-Pendulum geometric constraint: the geometric binding between the cog of the pendulum and the ball, establishes that the lenght between the two cog is time-invariant w.r.t. Σ_P. This constraint is summarized in the following equation:

$$\Gamma_B^E = \Gamma_P^E + R_P^E l, \tag{21}$$

it leads to 2 binding equations, the first concerning relations beween system's velocities and the second concerning relations between system's accelerations. The velocity constraint is the time derivative of (21), it gives:

$$\dot{\Gamma}_B^E = R_P^E R_B^P V_B = \dot{\Gamma}_P^E + \frac{d}{dt}(R_P^E l), \tag{22}$$

whereas, recalling the first equation of (6) and $\dot{R}_P^E V_P = R_P^E(\omega_p \times V_P)$ it becames:

$$R_B^P V_B = V_P + \omega_P \times l. \tag{23}$$

In the same way, the acceleration constraint is the time derivative of (23):

$$\frac{d}{dt}(m_B R_B^P V_B) = m_B(\dot{V}_P + \dot{\omega}_P \times l) \tag{24}$$

which becomes:

$$R_B^P(\omega_B^* \times V_B + \dot{V}_B) = (\dot{V}_P + \dot{\omega}_P \times l). \tag{25}$$

The further equation (25) is the dynamic constraint related to the ball-pendulum geometric constraint.

2) Ball's rolling constraint: a rolling without slipping constraint [9] has been assumed for the motion of the ball on the floor, it is a non-holonomic constraint that force the ball to have only pure rolling motion. Two binding equations are generated by this constraint, they are related to the tangential acceleration of the ball and to its angular acceleration. The pure rolling equation is $V_B = \omega_B \times R_B$, it generates:

$$\dot{V}_B = \dot{\omega}_B \times R_B \Rightarrow \dot{p}_B = -\frac{\dot{v}_B}{R_B}, \quad \dot{q}_B = \frac{\dot{u}_B}{R_B} \tag{26}$$

where $R_B = [0\,0\;-R_b]^T$ and R_b is the radius of the ball.

D. External Forces and Torques

The considered external forces are interaction forces which can be potential and no-potential.

1) Potential-forces: the potential force acting on the pendulum's rigid bodies and the ball are just the gravitational ones (g). In the analysis it is respectively referred to the pendulum and the ball frames, as G_P^E and G_B^E:

$$G_P^E = \begin{bmatrix} 0 & 0 & -m_p g \end{bmatrix}^T, \quad G_B^E = \begin{bmatrix} 0 & 0 & -m_b g \end{bmatrix}^T \tag{27}$$

2) Non-Potential forces: they are the external forces acting on the system, the reaction forces and the motor torques. The motor torque is an input for the system but it is also a non-potential force. The considered reaction forces $R_v = [r_{vx},\, r_{vy},\, r_{vz}]^T$ describes the interaction between ball and pendulum. It is applied to the cog of the ball and referred to Σ_P. This vector is used according to the Lagrange multiplier of the equation (21), allowing the definition of the external force and torques. In particular, the total external forces and torques acting on the pendulum are:

$$\begin{cases} {F_{ext}}_P^P = (R_P^E)^T G_P^E + R_v \\ {\tau_{ext}}_P^P = L \times R_v - U, \end{cases} \tag{28}$$

where $L = [0\,0\,-l]^T$ is the vector that identifies the cog of the ball referred to Σ_P. As before, calling $R_t = [r_{t_x}\, r_{t_y}\, r_{t_z}]^T$ the reaction force between the ball and the ground, the external force and torque acting on the ball are:

$$\begin{cases} {F_{ext}}_B^P = (R_P^E)^T (G_P^E + R_t) - R_v \\ {\tau_{ext}}_B^P = (R_P^E)^T(-R_B \times R_t) + U \end{cases} \tag{29}$$

VII. Non Linear System Dynamics

The non linear equations of motion are obtained by substituting (28) and (29) in (11), (14), (17), (20) and introducing all the constraints. The result is:

$$\begin{cases} m_p(\omega_P \times V_P + \dot{V}_P) = (R_P^E)^T G_P^E + Rv \\ (\omega_P \times I_P \omega_P + I_P \dot{\omega}_P) = L \times R_v + U \\ m_b(\omega_P \times (R_B^P V_B) + R_B^P(\omega_B^* \times V_B + \dot{V}_B)) = \\ = (R_P^E)^T (G_P^E + R_t) - R_v \\ \omega_P \times R_B^P I_B \omega_B + R_B^P(\omega_B^* \times I_B \omega_B + I_B \dot{\omega}_B) \\ = (R_P^E)^T(-R_B \times R_t) - U \\ R_B^P(\omega_B^* \times V_B + \dot{V}_B) = (\dot{V}_P + \dot{\omega}_P \times L) \\ \dot{p}_B = -\dfrac{\dot{v}_B}{R_b} \\ \dot{q}_B = \dfrac{\dot{u}_B}{R_b} \\ \dot{\omega}_B = 0 \end{cases} \tag{30}$$

The system (30) is a set of nonlinear algebric equations. The first two equations describe the pendulum dynamic subjected to the input U, the potential force G_P^E and the reaction force R_V. The second two equations describe the ball dynamic including the effect of the reaction force R_t. The fifth equation defines the geometric constraint between the ball and the pendulum, while three equations define the pure rolling condition of the ball. The system (30) can be solved w.r.t. the variables $[\dot{V}_P\, \dot{\omega}_P\, \dot{V}_B\, \dot{\omega}_B\, R_v\, R_t]$, its solution generates a set of equations each having thousand of terms. This solution is not useful for control purposes although it can be used for model simulation. Because of the complexity of this system, the nonlinear dynamic equations cannot be simplified in simple way for applying directly nonlinear control techniques. In literature some nonlinear control techniques have been proposed only by using simplified models with a-priori decoupling assumptions. This paper proposes the analysis of the linearized version.

VIII. Linear System Dynamics

In order to find the state space representation of the linearized system, the linear state vector $X = [\phi,\, p,\, \theta,\, q,\, \psi,\, r,\, \phi_b,\, p_b,\, \theta_b,\, q_b,\, x_b,\, u_b,\, y_b,\, v_b]^T$ and the input vector $U = [u_1,\, u_2,\, u_3]$ are introduced. The ball's variables r_B and $\dot{r}_B$ (respectively the angular position and velocity of the ball around its $\widehat{k}_B$ axis of Σ_B) are ignored because not relevant for the modelling purposes. The system (30) is linearized around the operating point with all states at zero, i.e. the unstable equilibrium point of the pendulum where the robot stands in a steady-state. This neutral point is a reasonable trade-off because the ballbot can tilt in any direction. The linearization leads to the following linear state-space representation:

$$\dot{X} = A\,X + B\,U, \quad y = C\,X, \tag{31}$$

where the system's matrices can be written as:

$$A=\begin{bmatrix}0&1&0&0&0&0&0&0&0&0&0&0&0&0\\a_{2,1}&0&0&0&0&0&0&0&0&0&0&0&0&0\\0&0&0&1&0&0&0&0&0&0&0&0&0&0\\0&0&a_{4,3}&0&0&0&0&0&0&0&0&0&0&0\\0&0&0&0&0&1&0&0&0&0&0&0&0&0\\0&0&0&0&0&0&0&0&0&0&0&0&0&0\\0&0&0&0&0&0&0&1&0&0&0&0&0&0\\a_{8,1}&0&0&0&0&0&0&0&0&0&0&0&0&0\\0&0&0&0&0&0&0&0&0&1&0&0&0&0\\0&0&a_{10,3}&0&0&0&0&0&0&0&0&0&0&0\\0&0&0&0&0&0&0&0&0&0&0&1&0&0\\0&0&a_{12,3}&0&0&0&0&0&0&0&0&0&0&0\\0&0&0&0&0&0&0&0&0&0&0&0&0&1\\a_{14,1}&0&0&0&0&0&0&0&0&0&0&0&0&0\end{bmatrix} B=\begin{bmatrix}0&0&0\\b_{2,1}&b_{2,2}&b_{2,2}\\0&0&0\\0&b_{4,2}&-b_{4,2}\\0&0&0\\b_{6,1}&b_{6,1}&b_{6,1}\\0&0&0\\b_{8,1}&b_{8,2}&b_{8,2}\\0&0&0\\0&b_{10,2}&-b_{10,2}\\0&0&0\\0&b_{12,2}&-b_{12,2}\\0&0&0\\b_{14,1}&b_{14,2}&b_{14,2}\end{bmatrix}. \tag{32}$$

The matrices A and B have the coefficients $a_{i,j}$ and $b_{i,j}$, $i = 1 \dots 14$, $j = 1 \dots 3$ showed in:

$$\begin{cases} a_{2,1} = a_{4,3} \triangleq a = \dfrac{glm_p[I_b + R_b^2(m_b+m_p)]}{I_p[I_p + R_b^2(m_b+m_p)] + l^2 m_p(I_b + R_b^2 m_b)} \\ a_{8,1} = a_{10,3} \triangleq \tilde{a} = \dfrac{-glm_p(R_b m_p l)}{I_p[I_b + R_b^2(m_b+m_p)] + l^2 m_p(I_b + R_b^2 m_b)} \\ a_{12,3} \triangleq \hat{a} = R_b \tilde{a} \quad a_{14,1} = -\hat{a} \quad b_{14,2} = \dfrac{1}{2}\hat{b} \\ b_{2,1} \triangleq b = \dfrac{R_b \cos\alpha[I_b + R_b^2(m_b+m_p) + R_b l m_p]}{R_w\{I_p[I_b + R_b^2(m_b+m_p)] + l^2 m_p(I_b + R_b^2 m_b)\}} \\ b_{2,2} = -\dfrac{1}{2} \quad b_{4,2} = \dfrac{\sqrt{3}}{2}b \quad b_{6,1} \triangleq \bar{b} = \dfrac{-R_b \sin\alpha}{R_w I_{p_z}} \\ b_{8,1} \triangleq \tilde{b} = \dfrac{-R_b\cos\alpha[I_p + m_p l(l+R_b)]}{R_w\{I_p[I_b + R_b^2(m_b+m_p)] + l^2 m_p(I_b + R_b^2 m_b)\}} \\ b_{8,2} = -\dfrac{1}{2}\tilde{b} \quad b_{10,2} = \dfrac{\sqrt{3}}{2}\tilde{b} \quad b_{12,2} = \dfrac{\sqrt{3}}{2}\hat{b} \quad b_{14,1} \triangleq -\hat{b} = -R_b\tilde{b} \end{cases} \tag{33}$$

Assuming a full state measurable by sensors, the matrix C is a 14×14 identity matrix. Unlike other different models, all the coefficients $a_{i,j}$ and $b_{i,j}$ are known in closed form, in terms of the system's physical parameters without resorting to numerical solutions. Furthermore no a-priori assumption about the decoupling of motion in the different planes have been made as is usually done in literature. The matrix A is a sparse matrix where the rows in even position contain the dynamic coefficients. Notice that the 6^{th} row of A is a null row: the pendulum yaw rate does not depend on the system dynamic. Hence, the yaw rate variable can be deleted in the state space model. This subsystem, then can be decoupled from the other equations, it has no dynamic and it only depends on the inputs. It can be easily shown that the linearized system has controllability and observability matrices with no full rank. This is because the last four equations of (31) describe the translational dynamic of the ball and depend linearly only on the roll and pitch dynamic described by the first four equations. Hence, the ball translation dynamic became a subsystem depending on the pendulum dynamic. In that case the controllability and observability matrices of the 10×10 system has full rank, then the system is fully controllable and observable and thus stabilizable. In order to simplify the system's analysis we propose to rewrite (32) as:

$$\begin{cases} \dot{p} = a\phi + bu_1 - \dfrac{1}{2}bu_2 - \dfrac{1}{2}bu_3 \\ \dot{q} = a\theta + \dfrac{\sqrt{3}}{2}bu_2 - \dfrac{\sqrt{3}}{2}bu_3 \\ \dot{r} = \bar{b}u_1 + \bar{b}u_2 + \bar{b}u_3 \\ \dot{p}_B = \tilde{a}\phi + \tilde{b}u_1 - \dfrac{1}{2}\tilde{b}u_2 - \dfrac{1}{2}\tilde{b}u_3 \\ \dot{q}_B = \tilde{a}\theta + \dfrac{\sqrt{3}}{2}\tilde{b}u_2 - \dfrac{\sqrt{3}}{2}\tilde{b}u_3 \\ \dot{u}_B = \hat{a}\theta + \dfrac{\sqrt{3}}{2}\hat{b}u_2 - \dfrac{\sqrt{3}}{2}\hat{b}u_3 \\ \dot{v}_B = -\hat{a}\phi - \hat{b}u_1 + \dfrac{1}{2}\hat{b}u_2 + \dfrac{1}{2}\hat{b}u_3. \end{cases} \tag{34}$$

Equation (34) shows how the nonlinear dynamics linearized at zero can be split in 4 subsystems of which 3 are independent: the yz-plane subsystem with roll dynamic $\dot{p}$ and $\dot{p}_B$; the pendulum yaw subsystem with dynamic $\dot{r}$; the xz-plane subsystem with the roll and pitch dynamics $\dot{q}$ and $\dot{q}_B$; a subsystem with dynamic $\dot{u}_B$ and $\dot{v}_B$ representing the ball translational equations of motion in the xy-plane of Σ_B. Under linear assumption this means that it is possible to control that system with three different controllers. Also it can be seen as the input (motors) exert different influence on each subsystem acting on each one in a linear combination. Notice that the yaw dynamic expressed by $\dot{r}$ is independent by all the other state variables, it depends only on the linear combination of the inputs, this means that it can be decoupled from the other dynamic behaviors.

IX. Conclusion

In this paper a new dynamical 3D-model for the Ballbot mechatronic system has been presented. It is based on a different approach with respect to the model already known in literature, since it uses the Newton-Euler method along with RPY angles instead of the Euler-Lagrange formalism. The complete nonlinear model has been linearized and further analyzed for control purposes. The linearized system has all its parameters known in terms of system's physical parameters without resorting to the numeric solutions. The results show that the model can be split in 4 subsystem in which 3 are independent. Attention has been also paid to the controllability problem. It has been shown that the yaw dynamics can be decoupled and the rest of the system is controllable. In this way the complexity of the system has been reduced, obtaining a more agile system. Further development are ongoing. The main goal is actually to propose a proper control based on this new linearized model, in respect with those proposed in literature. Other goals are to introduce the actuators dynamics in order to implement a voltage control instead of a torque control and apply a different kind of controller to the system.

References

[1] T. B. Lauwers, G. A. Kantor, R. L. Hollis. *A Dynamically Stable Single-Wheeled Mobile Robot with Inverse Mouse-Ball Drive*. Paper, Carnegie Mellon University, USA, 2006.

[2] U. Nagarajan, A. Mampetta, G. A. Kantor and R. L. Hollis. *State Transition, Balancing, Station Keeping, and Yaw Control for a Dynamically Stable Single Spherical Wheel Mobile Robot*. Paper, Carnegie Mellon University, USA, 2009.

[3] M. Kumagai and T. Ochiai. *Development of a Robot Balancing on a Ball*. Paper, Tohoku Gakuin University, Japan, 2008.

[4] J. Fong and S. Uppill. *Design and Build a Ballbot*. Report, The University of Adelaide, Australia, 2009.

[5] S. Leutenegger and P. Fankhauser. *Modelling and Control of a Ballbot*. Bachelor thesis, ETH Zurich (2010).

[6] U. Nagarajan, G. A. Kantor and R. L. Hollis. *The ballbot: An omnidirectional balancing mobile robot*. The International Journal of Robotics Research (2013).

[7] R. A. Garcia-Garcia and M. Arias-Montiel. *Linear Controllers for the NXT Ballbot with Parameter Variations Using Linear Matrix Inequalities*. IEEE control system 36(3) 121-136, 2016.

[8] King-Sun Fu, Rafael C. Gonzalez, C.S. George Lee. *Robotics Control, Sensing, Vision and Intelligence*. Book, McGraw-Hill, 1987.

[9] Ahmed A. Shabana. *Dynamics of multibody systems*. Book, Cambridge University Press, 2005.